

tation, and failure to thrive. Phenotypic severity correlates with the level of prelamin accumulation or lack of mature lamin A1 that result from mutations in *LMNA* (encodes lamin A/C) or *ZMPSTE24* (a zinc metalloproteinase that processes prelamin A to mature lamin A). Lamin is crucial for proper nuclear lamina formation. Subtypes A and B differ in the extent of lipodystrophy, age at presentation, and long-term sequelae.

Patients with MAD type A do not show characteristic syndromic features or partial lipodystrophy until age 4 or 5 years.<sup>1</sup>

MAD type B is rarer. To our knowledge, only 10 cases have been reported prior to the present one.<sup>1-6</sup> Compound heterozygous nonsense and missense mutations in *ZMPSTE24*<sup>1,3-5</sup> predominate, with 1 report of a homozygous missense mutation in *ZMPSTE24*<sup>6</sup> and 1 case of a homozygous null *ZMPSTE24* mutation combined with a “rescue” *LMNA* mutation.<sup>2</sup> Dysmorphic progeroid features, mottled pigmentation, and joint contractures present early in infancy. Skeletal dysplasias develop by age 1 to 2 years. Generalized lipodystrophy presents variably from the toddler to teen years. Metabolic disease is poorly defined but has been reported in young adulthood.

Two unique long-term sequelae for MAD type B are progressive glomerulopathy and subcutaneous calcified nodules. Clinically relevant kidney disease presents in patients who have reached their 20s,<sup>1,3,6</sup> but microhematuria with normal findings of kidney ultrasonography have been reported in early childhood.<sup>5</sup> Calcified nodules start as early as age 2 years.<sup>1</sup> Significantly, 2 patients in their late 20s or 30s have died from a combination of vascular calcifications and renal failure.<sup>3,6</sup>

Interestingly, though our patient has the same compound heterozygous mutation as was found in 2 other cases,<sup>2,3</sup> their clinical presentations are not identical. Indeed, neither *LMNA* or *ZMPSTE24* mutations were found in 3 other patients with MAD type B,<sup>1</sup> suggesting that undiscovered mutations may modulate the clinical phenotype.

Dermatologists may be consulted to evaluate dyspigmentation but can be instrumental in the diagnosis of MAD type B by recognizing its earlier multisystem constellation of symptoms. Earlier diagnosis would alert physicians of the particular need, among others, for early renal monitoring. However, disease heterogeneity suggests that management should be tailored to phenotypic severity.

**Julia M. Kwan, MD**

**Author Affiliation:** Department of Dermatology, Naval Health Clinic Hawaii, Pearl Harbor.

**Corresponding Author:** Julia M. Kwan, MD, Department of Dermatology, Naval Health Clinic Hawaii, 480 Central Ave, Pearl Harbor, HI 96860 (Julia.kwan@med.navy.mil).

**Published Online:** January 28, 2015. doi:10.1001/jamadermatol.2014.5068.

**Conflict of Interest Disclosures:** None reported.

**Disclaimer:** The views expressed in this article are those of the author and do not reflect the official policy or position of the Department of the Navy, Department of Defense, or the United States Government.

1. Agarwal AK, Fryns JP, Auchus RJ, Garg A. Zinc metalloproteinase, *ZMPSTE24*, is mutated in mandibuloacral dysplasia. *Hum Mol Genet.* 2003;12(16):1995-2001.

2. Shackleton S, Smallwood DT, Clayton P, et al. Compound heterozygous *ZMPSTE24* mutations reduce prelamin A processing and result in a severe progeroid phenotype. *J Med Genet.* 2005;42(6):e36.

3. Agarwal AK, Zhou XJ, Hall RK, et al. Focal segmental glomerulosclerosis in patients with mandibuloacral dysplasia owing to *ZMPSTE24* deficiency. *J Invest Med.* 2006;54(4):208-213.

4. Denecke J, Brune T, Feldhaus T, et al. A homozygous *ZMPSTE24* null mutation in combination with a heterozygous mutation in the *LMNA* gene causes Hutchinson-Gilford progeria syndrome (HGPS): insights into the pathophysiology of HGPS. *Hum Mutat.* 2006;27(6):524-531.

5. Miyoshi Y, Akagi M, Agarwal AK, et al. Severe mandibuloacral dysplasia caused by novel compound heterozygous *ZMPSTE24* mutations in two Japanese siblings. *Clin Genet.* 2008;73(6):535-544.

6. Ben Yaou R, Navarro C, Quijano-Roy S, et al. Type B mandibuloacral dysplasia with congenital myopathy due to homozygous *ZMPSTE24* missense mutation. *Eur J Hum Genet.* 2011;19(6):647-654.

## Edema and Telangiectasia of the Chest Caused by Neuroendocrine Carcinoma

Superior vena cava (SVC) syndrome includes a constellation of signs and symptoms resulting from SVC obstruction that produces elevated pressure in the afferent veins and increased blood flow through collateral vessels.

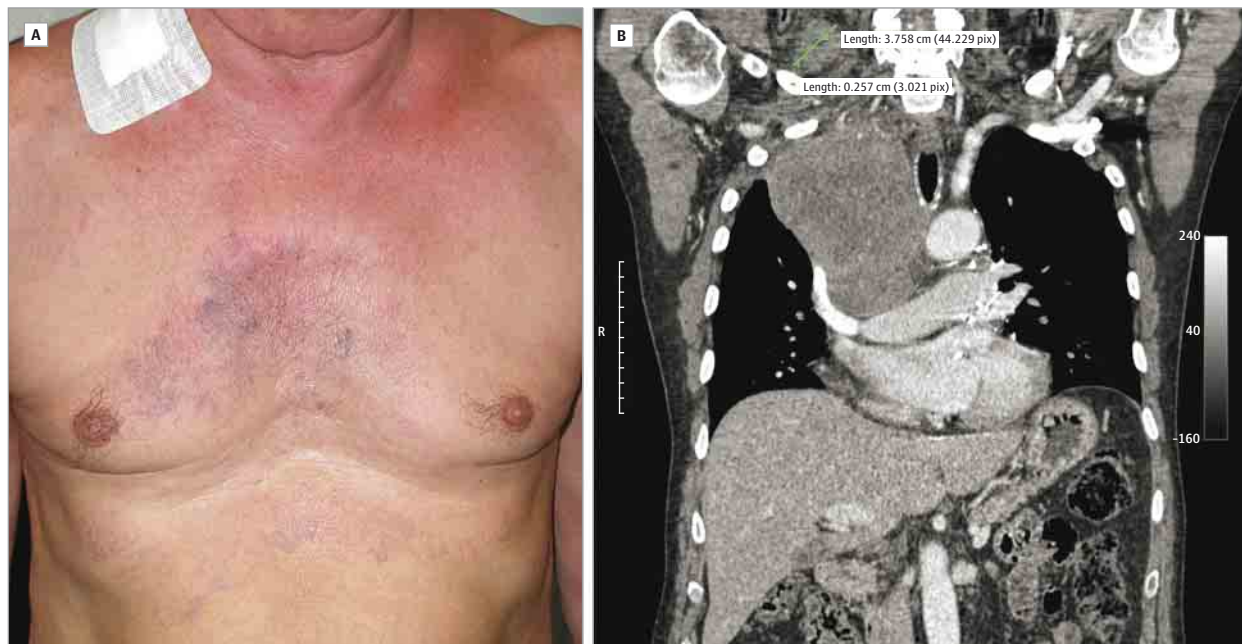
**Report of a Case |** A man in his 60s was referred for a subcutaneous nodule that had appeared in the right supraclavicular region about 1 year earlier. The patient, who had a 5-year history of chronic obstructive pulmonary disease, complained of hoarseness, cough, and tachycardia. At physical examination, the nodule, measuring about 4 cm in diameter, was round and fixed with irregular ill-defined margins. Edema and erythema of the neck area and a well-defined net of superficial dilated vessels in the thoracic and epigastric areas were also detected (**Figure 1A**).

Blood tests showed elevated levels of lactate dehydrogenase (1180 U/L; normal range, 250-500 U/L) and slightly raised levels of carcinoma antigen (CA) 15-3 (29 U/mL; normal range, 0-25 U/mL). Levels of CA 19-9, carcinoembryonic antigen, and  $\alpha$ -fetoprotein were within the normal range. Otolaryngology consultation revealed paralysis of the right vocal cord. Chest radiography showed an opaque thoracic mass approximately 12 cm in diameter located on the right apical side that caused left tracheal deviation. Thoracic computed tomography confirmed the presence of an expansive solid mass in the mediastinum infiltrating the right side of the trachea, the SVC, and the left brachiocephalic vein (**Figure 1B**). The mass also compressed the interazygos esophageal system, with vascular shunts detectable in the right paramediastinal side.

A punch biopsy of the nodule revealed a large-cell neuroendocrine carcinoma showing a proliferation of atypical medium and large undifferentiated cells and areas of necrosis and hemorrhage (**Figure 2A**). Immunohistochemical staining was positive for the neuroendocrine marker synaptophysin (**Figure 2B**). The diagnosis of mediastinal neuroendocrine carcinoma of unknown origin associated with SVC syndrome prompted referral for complete surgical excision. The patient died a few weeks later after multiple postsurgical complications.

**Discussion |** Historical causes of SVC syndrome are usually reported as infective, such as tuberculosis or syphilis. Cur-

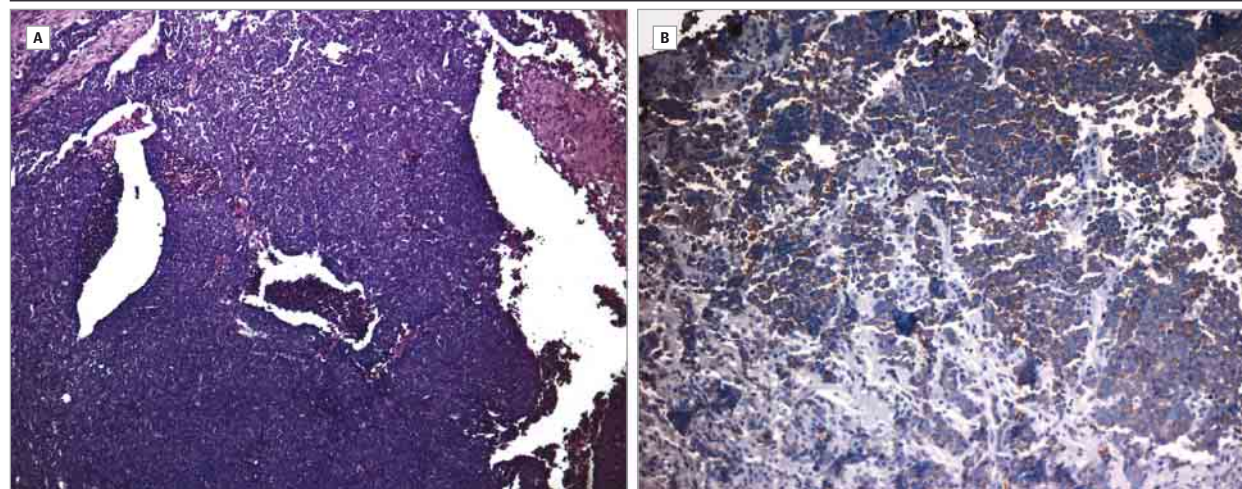
Figure 1. Superior Vena Cava Syndrome



A, Clinical view of edema and erythema of the neck and presence of a well-defined net of dilated vessels in the thorax and the epigastric region. B, Computed tomography of the chest showing an expansive solid mass involving

the mediastinum and infiltrating the right wall of the trachea, the superior vena cava and the left brachiocephalic vein; mass dimensions indicated by green lines.

Figure 2. Neuroendocrine Carcinoma Biopsy Specimens



A, Histopathology specimen showing a proliferation of atypical and undifferentiated cells of medium and large size and areas of necrosis and hemorrhage (hematoxylin-eosin, original magnification  $\times 100$ ). B, Under

synaptophysin immunohistochemical staining, specimen tested positive (original magnification  $\times 200$ ).

rently, in 60% to 90% of cases, the cause is determined to be a malignant condition, predominantly bronchopulmonary cancer (~85%), whereas causative benign conditions are less commonly reported and include mediastinal fibrosis, retrosternal goiter, lipomatous hypertrophy, and transvenous cardiac pacemakers.<sup>1,2</sup>

Superior vena cava syndrome is related to extrinsic compression or intraluminal stenosis of the SVC. Consequent collateral circulation depends on the level of the obstruction that

may be located (1) just at, (2) just above, or (3) just below the outlet of the azygos vein. In the first case, as in our case, dilated superficial collateral vessels are evident in the skin, involving internal mammary veins, epigastric veins, and intercostal veins. Signs and symptoms of SVC syndrome include facial or neck plethora, arm swelling, dilated chest veins, chest pain, dyspnea, light-headedness, dizziness, or syncope; presence of orthopnea and facial plethora may be exacerbated when the patient is supine.<sup>3,4</sup>

Mediastinal neuroendocrine carcinoma is one of the possible, although unusual, reported causes of SVC syndrome, with most patients showing a progressively worsening facial edema.<sup>5</sup> A case of SVC syndrome due to mediastinal carcinoid tumor has been previously reported in a 36-year-old man who presented with facial swelling, mild dyspnea, pain in the right arm, slurring of the voice, and deviation of the tongue to the left side.<sup>6</sup> However, development of cutaneous varicosities with multiple dilated venules on the anterior thoracic wall, as in this present report, has not been previously described to our knowledge in patients with mediastinal neuroendocrine carcinoma.

Recognition of SVC syndrome may be crucial for revealing a possible underlying malignant condition. In this regard, the dermatologist may play a decisive role because cutaneous manifestations may suggest this diagnosis when systemic symptoms are still lacking or negligible.

Francesco Lacarrubba, MD

Maria Rita Nasca, MD, PhD

Barbara Cammisuli, MS

Giuseppe Micali, MD

**Author Affiliations:** Dermatology Clinic, University of Catania, Catania, Italy.

**Corresponding Author:** Giuseppe Micali, MD, Dermatology Clinic, University of Catania, AOU "Policlinico-Vittorio Emanuele," PO "Gaspere Rodolico," Via S. Sofia 78, 95123 Catania, Italy (cldermct@nti.it).

**Published Online:** January 14, 2015. doi:10.1001/jamadermatol.2014.4988.

**Conflict of Interest Disclosures:** None reported.

1. Wilson LD, Dettnerbeck FC, Yahalom J. Clinical practice: superior vena cava syndrome with malignant causes. *N Engl J Med*. 2007;356(18):1862-1869.
2. Musumeci ML, De Pasquale R, Tedeschi A, Neri S, Micali G. Nonmalignant superior vena cava syndrome. *Int J Dermatol*. 2000;39(12):934-936.
3. Rice TW, Rodriguez RM, Light RW. The superior vena cava syndrome: clinical characteristics and evolving etiology. *Medicine (Baltimore)*. 2006;85(1):37-42.
4. Wan JF, Bezjak A. Superior vena cava syndrome. *Hematol Oncol Clin North Am*. 2010;24(3):501-513.
5. Maeda A, Nakata M, Yasuda K, et al. Unknown primary large cell neuroendocrine carcinoma (LCNEC) in the mediastinum. *Gen Thorac Cardiovasc Surg*. 2013;61(9):542-545.
6. Aggarwal P, Sharma SK, Chattopadhyay TK, Mukhopadhyay AK. Mediastinal carcinoid tumour with unusual manifestations. *Postgrad Med J*. 1989;65(763):327-328.

### Massive Subcutaneous Masses on the Back Related to $\beta_2$ -Microglobulin Amyloidosis

Patients undergoing dialysis are unable to properly eliminate  $\beta_2$ -microglobulin, a component of major histocompatibility complex, type 1, which is catabolized in the kidney. Accumulation of  $\beta_2$ -microglobulin favors the formation of amyloid, the deposition of which causes dialysis-related amyloidosis (DRA). Symptoms are initially osteoarticular, but progression of the disease involves systemic manifestations including cutaneous ones.

**Report of a Case** | A woman in her 50s presented with a history of subcutaneous masses on her back that she had noticed 8 years previously and that were producing postural discomfort. History included hepatitis C infection 23 years earlier and bilateral nephrectomy requiring treatment with dialysis for the

Figure 1. Clinical Appearance of the Back of the Patient



Three massive, elongated, parallel, skin-colored subcutaneous masses.

last 31 years. After 20 years of hemodialysis, she developed bilateral carpal tunnel syndrome and flexion contractures on her fingers; hence, she was diagnosed with DRA.

On physical examination, she was found to have 3 massive nodules projecting from her back, each with an elongated shape (Figure 1). The largest (measuring about 31.0 × 5.5 × 4.5 cm) was located over her spine, and the others (each measuring about 27.0 × 2.5 × 1.0 cm) were located symmetrically on either side of the spine. These masses had firm consistency and were covered by normal skin. Computed tomography revealed infiltration of subcutaneous fat without evidence of calcification. Examination also revealed macroglossia and some yellowish nodules (about 2-4 mm each) on the sides of her tongue.

Skin biopsy of the central mass of her back was performed demonstrating subcutaneous deposition of amorphous eosinophilic material (Figure 2A). The deposits stained positive with Congo red, showing apple-green birefringence under polarization. Immunostaining of the amorphous material was positive for  $\beta_2$ -microglobulin amyloid (Figure 2B).

**Discussion** | Up to 65% of patients undergoing dialysis for more than 10 years develop DRA, and the prevalence increases over the years.<sup>1</sup> Unlike other types of systemic amyloidosis, amyloid deposition in the skin or subcutaneous fat is extremely rare.<sup>2,3</sup> However, 3 types of cutaneous manifestations related